J Inorg Organomet Polym (2016) 26:536–544
DOI 10.1007/s10904-016-0340-8

Preparation and Characterization of Novel Hybrid Nanocomposites by Free Radical Copolymerization of Vinyl pyrrolidone with Incompletely Condensed Polyhedral Oligomeric Silsesquioxane

Ali Akbari[1] · **Nasser Arsalani**[1]

Received: 6 December 2015 / Accepted: 4 February 2016 / Published online: 15 February 2016

Abstract A new series of hybrid nanocomposites based on poly (vinyl pyrrolidone) (PVP) containing incompletely condensed polyhedral oligomeric silsesquioxane (IC-POSS) with different percentages of POSS were prepared via free radical copolymerization. Incompletely condensed, phenyl-POSS ($Na_3O_{12}Si_7(C_6H_5)_7$) with the highly reactive group of trisodium silanolate was used to prepare desire IC-POSS by nucleophilic substitution reaction. The products were characterized by Fourier transform infrared, X-ray diffraction, scanning electron microscopy, differential scanning calorimetry and thermogravimetric analysis techniques. The results of analysis confirmed that there are good interactions between IC-POSS and the PVP matrix. The thermal stability of the PVP was enhanced with the addition of small amounts of nano-filler. The solubility of the nanocomposites has been also tested and the results showed that with increasing the IC-POSS content the hydrophobicity of nanocomposites were increased.

Keywords Hybrid nanocomposites · Poly (vinyl pyrrolidone) · Free radical polymerization · Thermal properties · Incompletely condensed polyhedral oligomeric silsesquioxane (IC-POSS)

✉ Nasser Arsalani
arsalani@tabrizu.ac.ir

[1] Research Laboratory of Polymer, Department of Organic and Biochemistry, Faculty of Chemistry, University of Tabriz, Tabriz, Iran

1 Introduction

In the past decades considerable efforts have been devoted to the preparation and application of organic–inorganic hybrid nanocomposites because they combine the advantages of both traditional organic polymers and inorganic material moieties [1–3]. Therefore, academic and industrial interests of these nanomaterials in a number of areas such as medicine, energy, biology, optics, catalysis and sensors have been progressively increased [4]. Until now, in order to prepare organic–inorganic hybrid nanocomposites, various methods such as sol–gel techniques, post-treatment of organic polymers and copolymerization with hybrid building blocks have been developed [2]. Many inorganic nanosized building blocks involving clay layered silicates, transition metal oxides, carbon nanotubes, and so forth have been reported but SiO_2 is mentioned as being very substantial [5, 6].

Among hybrid organic/inorganic building blocks, polyhedral oligomeric silsesquioxanes (POSS) have attracted a significant research effort because of its unique properties such as definite size, rigid structure, well-dispersed ability in the hybrid polymers even on a molecular level and possessing organic functional groups in the eight corners. This inorganic framework with cubic structure is made up of silicone and oxygen ($SiO_{1.5}$) and the cage can be thought of as the smallest spherical silica. POSS with a generic empirical formula $(RSiO_{1.5})_n$ with $n = 4, 6, 8, 10$ [7–10] is a type of nano-sized building blocks with 1–3 nm in diameter where the substituent groups (R), connected tightly with the cage can be hydrogen or some organic groups such as methyl, aryl, vinyl, phenyl or any organofunctional derivative from these organic groups [9–11]. POSS nanostructured chemicals can be easily incorporated into common polymer systems as nanofillers via

chemical bonds, or van der Waals interaction between substituent groups (R) and polymer.

Regarding to the structure, these compounds are usually subdivided into two groups: completely condensed silsesquioxanes (CC-POSS) and incompletely condensed silsesquioxanes (IC-POSS). Many studies on POSS containing nanocomposits have been made and the most published articles in POSS chemistry are about CC-POSS with different active functional groups. It worth to mention that the polarity or structure of mother polymers [12] and the number of the functional groups on CC-POSS yield important influence on thermal property of hybrid nanocomposites. The number of the functional groups on CC-POSS also determined the architecture type of CC-POSS based polymers [13]. For example in three dimensional network type [14–16], bead type [17, 18] and pendent type [19, 20] architectures the CC-POSS cages possess multi-functional polymerizable groups (more than two), two functional groups and single functional group respectively.

However, IC-POSS has many advantages of CC-POSS including high thermal resistance, lower dielectric constant and so forth. The active groups of the most IC-POSS derivatives are silanol or sodium silanolate groups, which are not suitable to participate in copolymerization with other monomers, so it is necessary to convert these groups to vinyl or allyl groups [7].

For the first time Guozheng Liang and coworkers [21] have synthesized a new incompletely condensed POSS containing three reactive allyl groups (TAP-POSS) in moderate yields. For simplicity, it was assigned as TAP-POSS. (Figure 1).

They used TAP-POSS in order to develop thermal stability and dielectric properties of bismaleimid resins. Till now, there are a few reports about the effect of IC-POSS on the thermal properties of polymers [9, 22–24].

From a material science point of view, poly (vinyl pyrrolidone) (C_6H_9NO) (PVP) is one of the most important polymers made from the *N*-vinylpyrrolidone as monomer. Having many excellent properties such as non-toxic, physiologically compatible, hydrophilic nature, transparency, non-ionic, essentially chemically inert and colorless made it suitable for numerous applications in medicine pharmaceutical technology, cosmetic and in the technical industry [25, 26]. In a mass of past studies, many different types of nanofiller were integrated into the PVP [27–30] but incorporation of POSS as three-dimensional nanofiller into the PVP is rare [31].

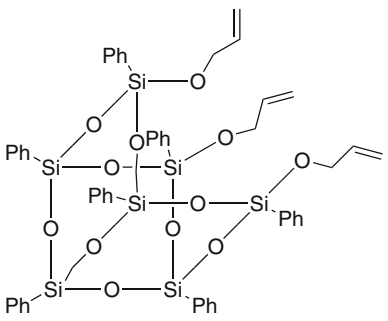

Fig. 1 Structure of TAP-POSS

To the best of our knowledge, there has been no precedent report on the use of TAP-POSS in the preparation of hybrid nanocomposits with other vinylated monomers. In continuation of our study on the POSS chemistry [32], for the first time incompletely condensed POSS containing three reactive allyl groups (TAP-POSS) was copolymerized with *N*-vinyl pyrrolidone to prepare novel organic–inorganic hybrid nanocomposits with different feed ratio of TAP-POSS which assigned as PVP–TAP-$POSS_n$ where n = 5, 7, 10 and 15 exhibiting the TAP-POSS wt%, which are characterized with Fourier transform infrared spectroscopy (FT-IR), X-ray diffraction (XRD), scanning electron microscopy (SEM), thermogravimetric analysis (TGA) and differential scanning calorimetry (DSC) techniques.

2 Experimental

2.1 Materials

N-vinylpyrrolidone (98 %) and allyl bromide was purchased from Sigma-Aldrich, phenyltrimethoxysilane [$C_6H_5Si(OCH_3)_3$; 98 %] was supplied from Acros, azobis(isobutyronitrile) (AIBN) was also from Sigma-Aldrich and was recrystallized from methanol before use. Sodium hydroxide (NaOH) was purchased from Merck Co. Solvents such as tetrahydrofuran (THF), acetone, acetonitrile, *n*-hexane and toluene also were obtained from Merck Co. *N*-vinylpyrrolidone distilled on calcium hydride under reduced pressure prior to use.THF and toluene were dried by distillation over Na/benzophenone under a nitrogen atmosphere immediately before use.

2.2 Synthesis of Heptaphenyltricycloheptasiloxane Trisodium Silanolate (HPSTS) [$Na_3O_{12}Si_7(C_6H_5)_7$]

HPSTS was synthesized in our laboratory according to the procedures described by Fukuda et al. [33]. Briefly, a round-bottom flask equipped with a reflux condenser and a magnetic bar was loaded with phenyltrimethoxysilane (7.051 g, 35.620 mmol), deionized water (0.812 g, 45.160 mmol) and NaOH (0.616 g, 15.4 mmol) with 39 mL of THF. After refluxed for 5 h, the reaction mixture

was cooled down to room temperature and held at this temperature with vigorous stirring for additional 15 h. All the solvent and other volatile compounds were removed using rotary evaporator and the white solids were obtained. After dried at 60 °C in vacuum for 24 h, the product was obtained with the yield of 95.5 %. ^{1}HNMR (400 MHz, $CDCl_3$), δ: 6.91–7.42 (m, Ph–H). FT-IR (cm^{-1}, KBr): 3049, 1595, 1430, and 1132–1050 (Si–Ph), 1050–1000 (Si–O–Si).

2.3 Synthesis of TAP-POSS

For the first time the synthesis of TAP-POSS was reported by Liang et al. [21]. A two- step synthesis of TAP-POSS was outlined in Fig. 2. Typically, into a 250 ml three-necked flask equipped with a reflux condenser and a magnetic stirrer containing 100 ml anhydrous acetone, HPSTS (2 g, 2 mmol) was added and allowed to dissolve completely, then allyl bromide (1.45 g, 12 mmol) was quickly added to the solution with vigorous stirring. Reaction was carried out according to a regular thermal program, 30 °C/3 h + 50 °C/3 h + 60 °C/3 h, after that formation of the white solid (NaBr) indicated that the nucleophilic substitution was over. After filtration of NaBr, all the solvent and volatile compounds were removed using rotary evaporator to get a pale yellow viscous liquid; TAP-POSS was precipitated from distilled water. For more purification, the crude product washed with acetonitrile. The pale yellow solids were then dried in vacuum at 50 °C for 48 h to afford the product with a yield of 55 %. ^{1}HNMR (400 MHz, $CDCl_3$), δ: 7.10–7.51 (m, Ph–H), 4.47, 5.10, 5.84 ($–CH_2–CH=CH_2$). FT-IR (cm^{-1}, KBr): 3049, 2925, 2850, 1595, 1430, and 1132–1050 (Si–Ph), 1050–1000 (Si–O–Si).

2.4 Hybrid Nanocomposites Preparation

All polymerization reactions were carried out under nitrogen using a vacuum-line system, the poly (vinylpyrrolidone-co-TAP-POSS) $_n$ hybrid nanocomposits were prepared via one-step free-radical polymerization technique, as illustrated in Fig. 3. For comparison, a pure PVP was also synthesized. Taking PVP–TAP-$POSS_5$ as an example, the product was prepared as follows: 2.5 g of vinylpyrrolidone and 0.125 g of TAP-POSS monomer in 20 mL dried toluene were polymerized using an AIBN initiator (1 wt% based on monomer) at 70 °C under nitrogen atmosphere for 24 h. The product then was poured into excess *n*-hexane under vigorous stirring to precipitate the copolymer, then purified in THF/Cyclohexane and dried in a vacuum oven. A 66 % product yield was obtained through this procedure.

2.5 Measurements

Fourier transform infrared (FT-IR) spectra were recorded using a Bruker FTIR spectrometer (model Tensor 27) over the range of 400–3500 cm^{-1} using spectroscopic grade KBr powder at room temperature.

The SEM was used to observe the surface morphologies and dimensions of hybrid nanocomposits, and images were taken with an emission scanning electron microscope

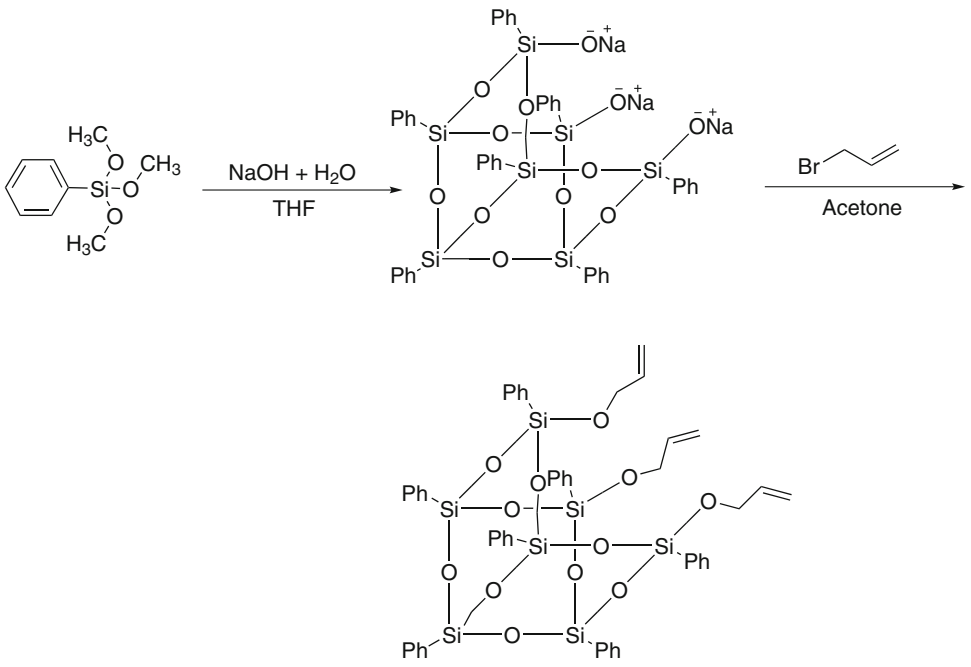

Fig. 2 The synthesis of TAP-POSS by nucleophilic substitution

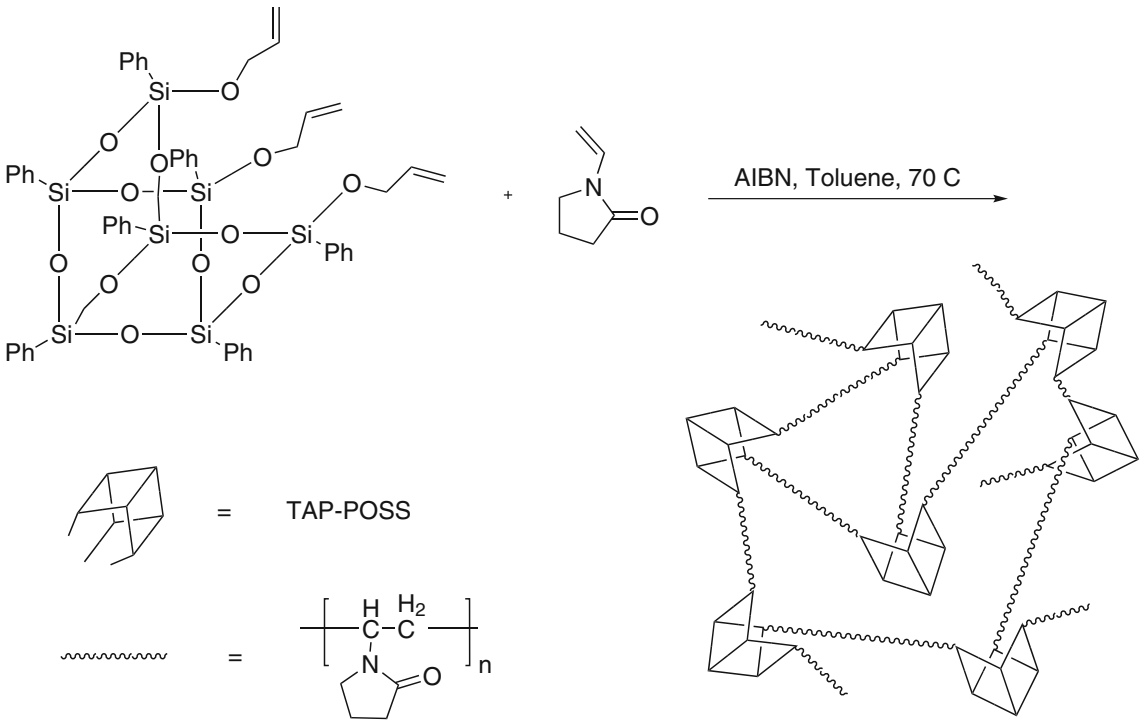

Fig. 3 Synthetic process of nanocomposites via radical polymerization

(MIRA3 FEG-SEM, Tescan, Czech) at an accelerating voltage of 30 kV with an energy-dispersive X-ray (EDX) spectroscopy.

Wide angle X-ray powder diffraction patterns (XRD) of the samples were obtained at room temperature on Siemens diffractometer (Siemens D-500, Germany) in the scan range of 2θ from 5° to 70°.

A differential scanning calorimeter (TA60, Shimadzu, Japan) was used to measure melting point of samples. The equipment was calibrated using indium and zinc. Each sample was carefully weighted (5 mg) into an aluminum pan and then hermetically sealed. Samples were heated ranging 25–350 °C at a scanning rate of 20 °C/min under nitrogen gas.

Thermogravimetric (TGA) analyses were performed using a Linseis L81A1750 (Germany) at a heating rate of 10 °C/min under high purity nitrogen atmosphere from 50 to 800 °C.

3 Results and Discussion

3.1 Structure Characterization of PVP–TAP-POSS$_n$ Nanocomposites

FT-IR spectroscopy is a powerful tool for structure elucidation. So in order to confirm the existence of TAP-POSS in the PVP–TAP-POSS nanocomposites, FT-IR spectra of pure TAP-POSS, PVP–TAP-POSS$_5$, PVP–TAP-POSS$_7$, PVP–TAP-POSS$_{10}$, PVP–TAP-POSS$_{15}$ and pure PVP are introduced in Fig. 4. The pure PVP shows two characteristic peaks at 1676 and 1228 cm^{-1}, which are assigned to C=O and C–N stretching vibrations, respectively. The stretching vibrations of methylene and methine groups are located at 2926 cm^{-1}. The pure POSS shows a strong and symmetric Si–O–Si stretching vibration at 1133 cm^{-1} [34] which is the characteristic peak of silsesquioxane cages. The spectra of all PVP–TAP-POSS nanocomposites are similar to that of the PVP except that a strong and symmetric peak appears at 1133 cm^{-1} in all the spectra, a characteristic Si–O–Si stretching of the silsesquioxane cage. In addition, the intensity of this vibration absorption increases with the increase of the POSS feed ratio, meaning that the POSS cage is indeed incorporated into the polymeric matrix [35]. Covalent bonds connections are formed between the organic and inorganic phases and led to increase the compatibility of the two phases.

3.2 Morphologies of PVP–TAP-POSS Hybrid Nanocomposites

The morphology and distribution of nanofillers in the mother polymer matrix is vitally important to the physical properties of the prepared nanocomposites. The SEM can be used to observe the cross-section fracture surfaces of hybrid nanocomposites. Figure 5a, b show SEM image and

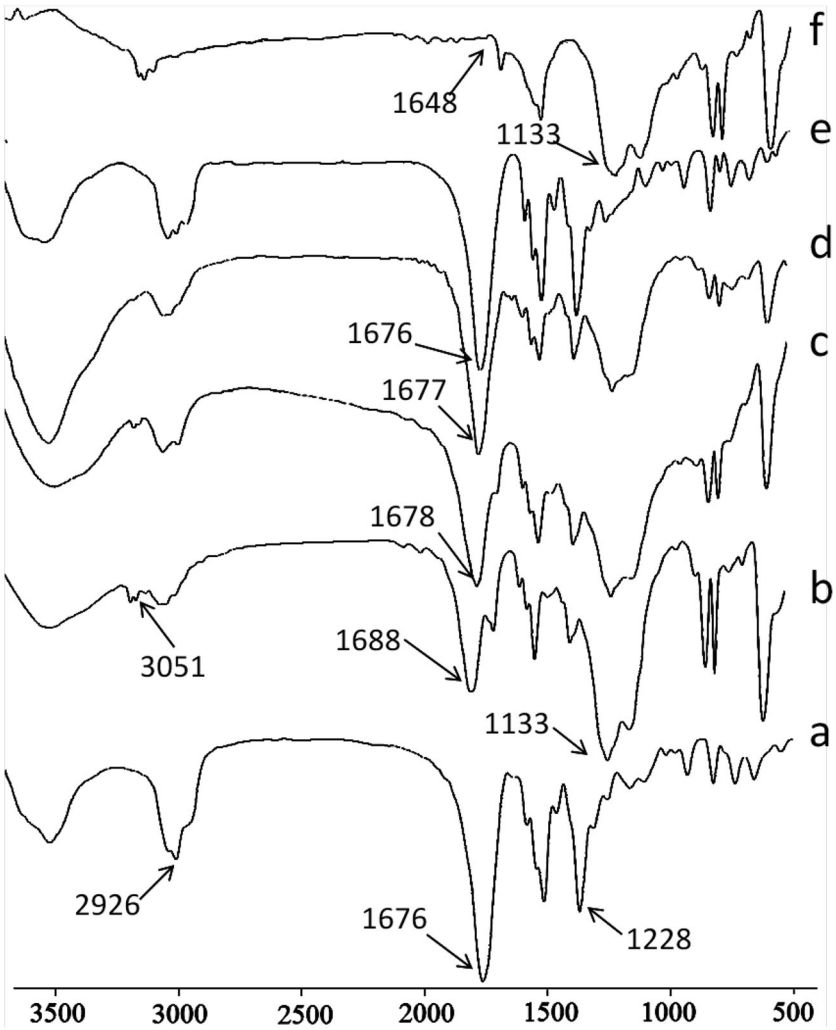

Fig. 4 FT-IR spectra for PVP–TAP-$POSS_n$ nanocomposites. *a* pure PVP; *b* PVP–TAP-$POSS_5$; *c* PVP–TAP-$POSS_7$; *d* PVP–TAP-$POSS_{10}$; *e* PVP–TAP-$POSS_{15}$; *f* TAP-POSS

EDX Si map of PVP–TAP-$POSS_7$ nanocomposite, respectively. In this case, 7 % POSS nanoparticles loading in nanocomposite or lower, there is no aggregation of POSS nanoparticles and the surface fracture was very smooth and homogeneous. Organic and inorganic phases were densely mixed without any obvious phase separation or gaps. In Fig. 5b, EDX Si map also demonstrated that the POSS nanofillers were homogeneously dispersed throughout the mother polymer matrices. This enhanced dispersion can be attributed to the existence of covalent bonds between TAP-POSS nanoparticles and the *N*-vinylpyrrolidone monomers. POSS nanoparticles have very small sizes (1–3 nm) so they could not be directly observed in SEM [36]. According to Fig. 5c, some POSS aggregations can be seen when the molar percentage of POSS in the nanocomposites was 10 % or higher [37]. In addition the solubility of control PVP and its nanocomposites with TAP-POSS is summarized in Table 1. PVP is known as very important water soluble polymer but the existence of TAP-POSS in PVP made the all nanocomposites insoluble in water. We have also tested the solubility of nanocomposites in other common organic solvents as shown in Table 1. The results indicated that the solubility of these hybrid nanocomposites was decreased with increasing the TAP-POSS weight percentages. This fact demonstrated that the synthesized hybrid nanocomposites with 10 and 15 % of TAP-POSS are possibly of network structure rather than of star-type structure since network nanocomposites are insoluble in any solvent [38, 39]. To confirm our presumption, we used a 0.22 μm membrane for filtration of all the as-synthesized solutions and then the filtered solutions were analyzed by GPC. The results showed that when the TAP-POSS content is more than 5 %, GPC does not display response of polymers, indicating that almost no polymeric substance passes through the membrane filter during filtration.

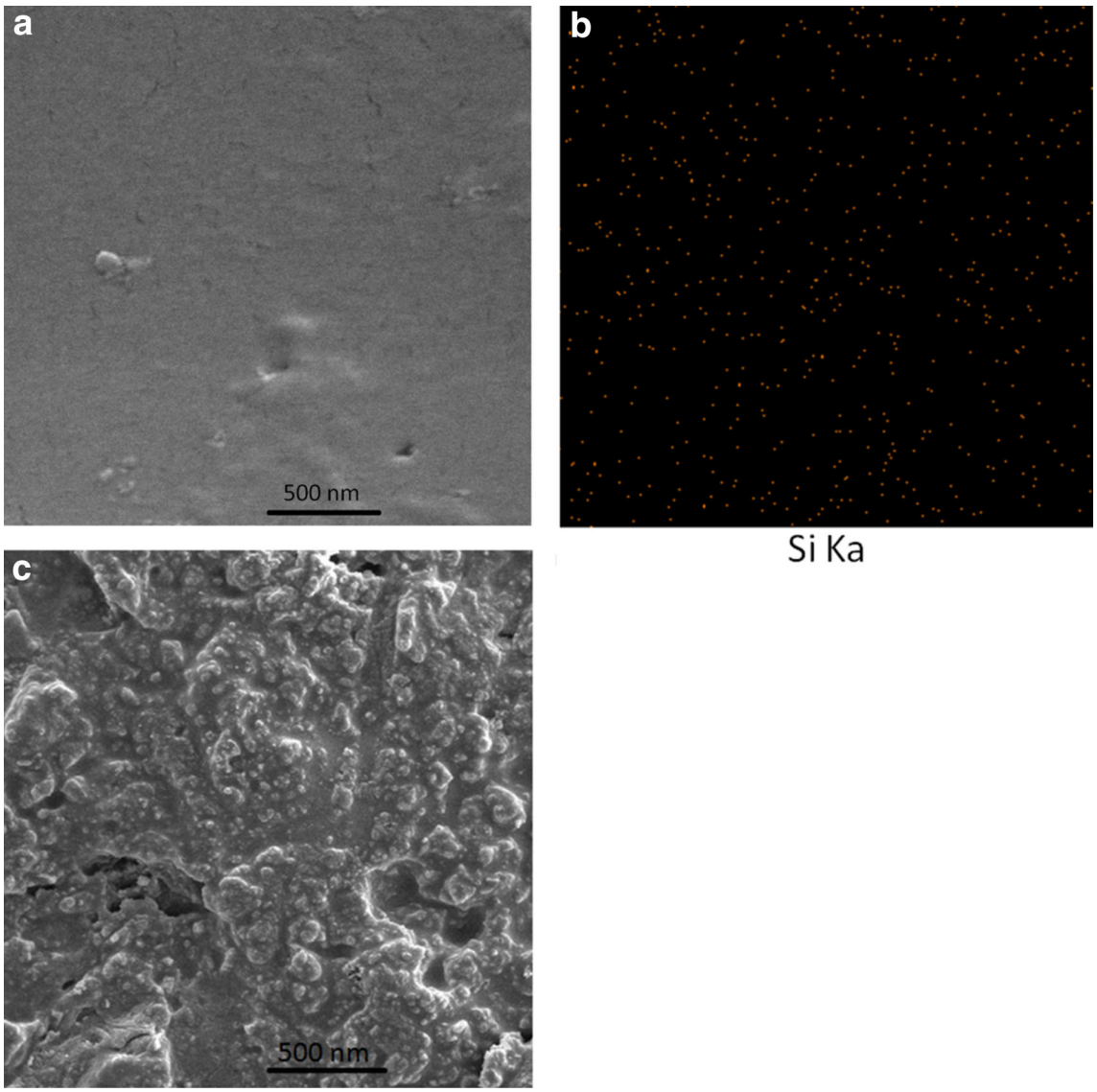

Fig. 5 **a** SEM image of PVP–TAP-POSS$_7$; **b** Si mapping of PVP–TAP-POSS$_7$ and **c** SEM image of PVP–TAP-POSS$_{10}$

Table 1 The solubility of nanocomposites in different solvent

Sample	Water	Acetone	THF	Chloroform	Dichloromethane	DMF	DMSO	Dioxane
PVP	+	−	−	+	+	+	+	+
PVP–TAP-POSS$_5$	−	−	−	+	+	+	+	+
PVP–TAP-POSS$_7$	−	−	−	−	−	−	−	−
PVP–TAP-POSS$_{10}$	−	−	−	−	−	−	−	−
PVP–TAP-POSS$_{15}$	−	−	−	−	−	−	−	−

(+) fully water soluble, (−) insoluble in water

3.3 XRD Analysis

XRD was used to further characterize the dispersion of the PVP–TAP-POSS$_n$ hybrid nanocomposites. Diffraction patterns of the pure TAP-POSS, PVP–TAP-POSS$_7$, PVP–TAP-POSS$_5$, pure PVP, PVP–TAP-POSS$_{10}$, and PVP–TAP-POSS$_{15}$ hybrid nanocomposites are shown in Fig. 6. The sharp crystalline peak appearing at about $2\theta = 7.0°$

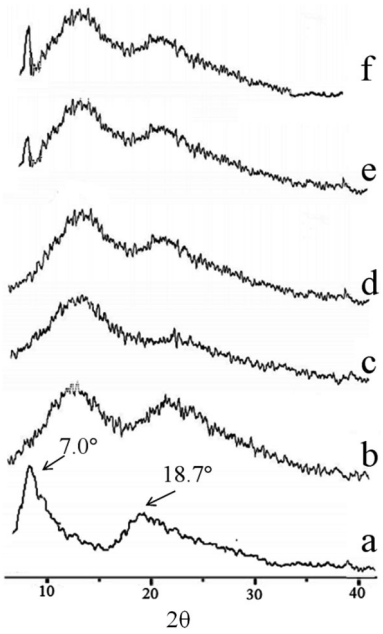

Fig. 6 XRD patterns of *a* TAP-POSS; *b* PVP–TAP-POSS$_7$; *c* PVP–TAP-POSS$_5$; *d* PVP; *e* PVP–TAP-POSS$_{10}$; *f* PVP–TAP-POSS$_{15}$

and the broad diffraction peak at about $2\theta = 18.7°$ are attributed to the cage-like structure and the amorphous structure of TAP-POSS respectively which are in close agreement with the literature results for TAP-POSS structure [21]. Existence of these peaks demonstrates that TAP-POSS is incompletely cage-like structure. Conversely, neat PVP exhibits a typical amorphous pattern. Considering Fig. 6, it comes out that the WAXD profiles of the samples PVP–TAP-POSS$_5$ and PVP–TAP-POSS$_7$, containing 5 and 7 wt% of TAP-POSS respectively turned out to be similar to that of neat PVP. So it can be resulted that TAP-POSS nanoparticles were dispersed very well in the polymer matrices and there is no any aggregation between POSS nanoparticles. In these cases we have also observed a shift in the location of the amorphous peak of the PVP, and the POSS nanoparticles will be expected to push polymer chains apart and shift the amorphous peak to the smaller angle [40] When the POSS weight percentage reaches 10 wt% a new peak matching the peak of the POSS at 7.0° (2θ) appears and becomes more prominent at TAP-POSS 15 wt%. The appearance of this characteristic diffraction peak in nanocomposite shows the TAP-POSS nanoparticles have aggregated. These results are in good agreements with our SEM results.

3.4 Thermal Properties

Incorporation of POSS nanobuildings in polymer structures has strong effects on thermal and physical properties of nanocomposites. The TGA and DSC techniques were used to study the thermal properties of the PVP–TAP-POSS$_n$. In many research reports, FT-IR data have been used to explain the Tg enhancement mechanism of POSS-based polymers [41–43]. The Tg values of the PVP–TAP-POSS$_n$ with different weight percentage of TAP-POSS are shown in Table 2. As it can be seen the PVP homopolymer has a Tg at 146 °C. With the increasing of POSS percentage the Tg of the nanocomposites increases gradually. As we mentioned the synthesized PVP–TAP-POSS nanocomposites have a network structure, and in these structures as shown in Fig. 3, TAP-POSS cores play as joint points which limit the free motion of PVP chains, resulting to the Tg enhancement. In another word increasing the TAP-POSS content means that increasing the joint points, leading in higher Tg. In our system when the TAP-POSS weight percentage is 15 % or higher we could not detect Tg due to very high crosslinkage that completely restricts the movements of PVP chains. Another important factor that causes improvement in Tg values is dipole–dipole interactions. These interactions happen between TAP-POSS cores and PVP chains. In order to study of these dipole–dipole interactions we used the FT-IR data of PVP–TAP-POSS nanocomposites. As it can be seen in Fig. 4, the PVP homopolymer has the characteristic carbonyl vibration at 1676 cm^{-1} and interestingly when the POSS content increases this carbonyl vibration was shifted to higher wavelength. For example when the POSS content is 15 % the carbonyl peak has maximum shift around 1688 cm^{-1}. This phenomenon shows that with the increasing of TAP-POSS content, the dipole–dipole interaction between TAP-POSS and PVP chains will be increased. In our nanocomposites, the hybrid structure (network structure) and dipole–dipole interactions have substantial roles in the enhancement of Tg. Tg improvements showed that TAP-POSS was covalently bonded to the PVP and can be dispersed homogenously in the copolymerized nanocomposites [42]. Basically the variation of Tg of POSS-containing polymers depends on many complicated factors such as hybrid structure, POSS loading and the type of POSS.

TGA thermograms of PVP–TAP-POSS$_n$ nanocomposites and pure PVP are illustrated in Fig. 7, and the related characteristic data obtained from these thermograms are summarized in Table 2. The thermal stability of the pure PVP was improved due to the incorporation of TAP-POSS into the PVP matrix homogenously. As it can be seen in Fig. 7, TGA curves for PVP and PVP–TAP-POSS$_5$ (5 % wt TAP-POSS) show two steps. First step may be associated with loss of adsorbed water in the PVP. It is worthwhile to mention that PVP is hygroscopic in nature therefore; it readily absorbs water from the surrounding. This weigh loss is 5 % for pure PVP and 3.21 % for hybrid nanocomposite when 5 % TAP-POSS was incorporated. First step disappeared when the TAP-POSS content is

Table 2 Effect of TAP-POSS feed ratio on the properties of PVP–TAP-POSS$_n$ nanocomposites

Sample	TAP-POSS (wt%)	T_g (°C)	T_{de} (°C)	Char yield (%)
PVP	0.00	146	388	10
PVP–TAP-POSS$_5$	5.00	151	400	12
PVP–TAP-POSS$_7$	7.00	156	411	16
PVP–TAP-POSS$_{10}$	10.00	162	420	18

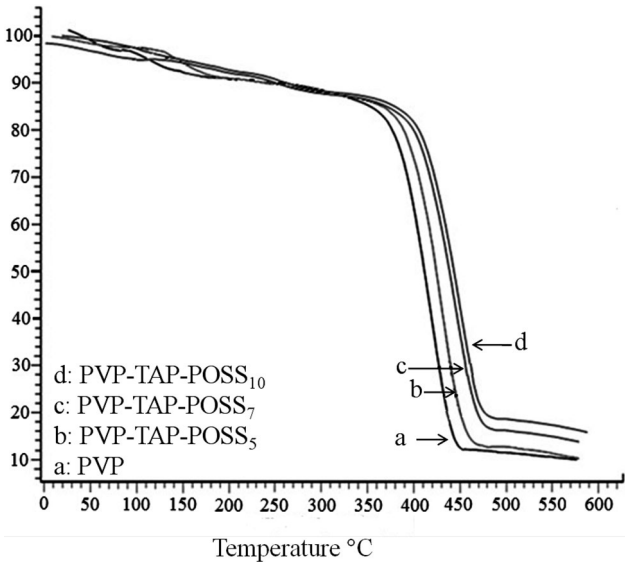

Fig. 7 The TGA thermograms of pure PVP and PVP–TAP-POSS$_n$ nanocomposites

higher than 5 %. These results showed that incorporation of TAP-POSS not only increased the thermal stability but also increased the hydrophobicity of hybrid nanocomposites. The second thermal degradation event took place at 388 °C for pure PVP and increased with IC-POSS incorporation. On the other hand for PVP–TAP-POSS$_n$ nanocomposites T_{de} and char yields increase with the increasing of POSS contents. All these data are summarized in Table 2.

4 Conclusion

Novel PVP nanocomposites containing IC-POSS were synthesized successfully using free radical polymerization. The structures of the PVP–TAP-POSS hybrid nanocomposites were characterized by FT-IR, XRD and SEM techniques. Incorporation of the TAP-POSS affected the solubility, thermal stability as well as the structure of the PVP. The solubility of nanocomposites has been also tested in water and various common organic solvents. Insolubility of these nanocomposites demonstrated the network structure rather than star or liner structures of nanocomposites. DSC and TGA techniques were used to evaluation of thermal property of hybrid nanocomposites and results showed an improvement in the thermal properties of hybrid nanocomposites.

Acknowledgments The authors would like to thank the Tabriz University for financially supporting this research.

References

1. W. Zhang, A.H.E. Müller, Prog. Polym. Sci. **38**, 1121 (2013)
2. H. Zou, S. Wu, J. Shen, Chem. Rev. **108**, 3893 (2008)
3. H. Yahyaei, M. Mohseni, H. Ghanbari, J. Inorg. Organomet. Polym. **25**, 1305 (2015)
4. L. Nicole, C. Boissiere, D. Grosso, A. Quach, C. Sanchez, J. Mater. Chem. **15**, 3598 (2005)
5. Y. Rao, S. Chen, Macromolecules **41**, 4838 (2008)
6. K. Daimatsu, H. Sugimoto, E. Nakanishi, T. Yasumura, K. Inomata, J. Appl. Polym. Sci. **109**, 1611 (2008)
7. D.B. Cordes, P.D. Lickiss, F. Rataboul, Chem. Rev. **110**, 2081 (2010)
8. G.Z. Li, L.C. Wang, H.L. Ni, C.U. Pittman, J. Inorg. Organomet. Polym. **11**, 123 (2001)
9. C.H. Su, Y.P. Chiu, C.C. Teng, C.L. Chiang, J. Polym. Res. **17**, 673 (2010)
10. W. Wang, W. Ding, J. Yu, M. Fei, J. Tang, J. Polym. Res. **19**, 9948 (2012)
11. H.U. Rehman, M.I. Sarwar, Z. Ahmad, H. Krug, H. Schmidt, J. Non-Cryst. Solids **211**, 105 (1997)
12. Y. Feng, Y. Jia, S. Guang, H. Xu, J. Appl. Polym. Sci. **115**, 2212 (2010)
13. H. Xu, S.W. Kuo, J.S. Lee, F.C. Chang, Polymer **43**, 5117 (2002)
14. W.Y. Chen, S.H. Ko, T.H. Hsieh, F.C. Chang, Y.Z. Wang, Macromol. Rapid Commun. **27**, 452 (2006)
15. Y.S. Ye, W.Y. Chen, Y.Z. Wang, J. Polym, Sci. Polym. Chem. **44**, 5391 (2006)
16. W.Y. Nie, G. Li, Y. Li, H.Y.C. Xu, Chem. Lett. **20**, 738 (2009)
17. S. Wu, T. Hayakawa, R. Kikuchi, S.J. Grunzinger, M. Kakimoto, Macromolecules **40**, 5698 (2007)
18. S. Wu, T. Hayakawa, M. Kakimoto, H. Oikawa, Macromolecules **41**, 3481 (2008)
19. C.M. Leu, Y.T. Chang, K.H. Wei, Chem. Mater. **15**, 3721 (2003)
20. Y.W. Chen, L. Chen, H.R. Nie, E.T. Kang, J. Appl. Polym. Sci. **99**, 2226 (2006)
21. L. Zeng, G. Liang, A. Gu, L. Yuan, D. Zhuo, J-t Hu, J. Mater. Sci. **47**, 2548 (2012)
22. H. Liu, S. Zheng, K. Nie, Macromolecules **38**, 5088 (2005)
23. K. Madhavan, D. Gnanasekaran, B.S.R. Reddy, J. Appl. Polym. Sci. **114**, 3659 (2009)
24. H. Bai, Y. Zheng, R. Yang, A. Zhang, N. Wang, Polym. Compos. (2015). doi:10.1002/pc.23628
25. A. Bahari, M. Roodbari Shahmiri, M. Derahkshi, M. Jamali, J Nanostruct. **2**, 313 (2012)
26. H. Folttmann, A. Quadir, Drug Deliv. Technol. **8**, 22 (2008)

27. G. Carotenuto, G.P. Pepe, L. Nicolais, Eur. Phys. J. B **16**, 11 (2000)
28. H.K. Hong, C.K. Park, M.S. Gong, Bull. Korean Chem. Soc. **31**, 1252 (2010)
29. J. Puisŏ, D. Adliene, A. Guobiene, I. Prosycevas, R. Plaipaite-Nalivaiko, Mater. Sci. Eng. B **176**, 1562 (2011)
30. O.J. Ilegbusi, H. Song, R. Chakrabarti, J. Bionic Eng. **7**, S30 (2010)
31. H. Xu, S.W. Kuo, J.S. Lee, F.C. Chang, Macromolecules **35**, 8788 (2002)
32. A. Akbari, N. Arsalani, M. Amini, E. Jabbari, J. Mol. Catal. A **414**, 47 (2016)
33. K. Koh, S. Sugiyama, T. Morinaga, K. Ohno, Y. Tsujii, T. Fukuda, M. Yamahiro, T. Iijima, H. Oikawa, K. Watanabe, T. Miyashita, Macromolecules **38**, 1264 (2005)
34. H. Mori, M.G. Lanzendofer, A.H.E. Muller, J.E. Klee, Macromolecules **37**, 5228 (2004)
35. H. Xu, S.W. Kuo, C.F. Huang, F.C. Chang, J. Polym. Res. **9**, 239 (2002)
36. J. Duan, E. Litwiller, I. Pinnau, J. Membr. Sci. **473**, 157 (2015)
37. J-t Hu, A. Gu, Z. Jiang, G. Liang, D. Zhuo, L. Yuan, B. Zhang, X. Chen, Polym. Adv. Technol. **23**, 1219 (2012)
38. Y. Gao, C. He, F.-L. Qing, J. Polym. Sci. Part A **49**, 5152 (2011)
39. H. Xu, B. Yang, J. Wang, S. Guang, C. Li, J. Polym. Sci. Part A **45**, 5308 (2007)
40. E.T. Kopesky, T.S. Haddad, G.H. McKinley, R.E. Cohen, Polymer **46**, 4743 (2005)
41. B. Yang, J. Li, J. Wang, H. Xu, S. Guang, C. Li, J. Appl. Polym. Sci. **111**, 2963 (2009)
42. Y. Feng, Y. Jia, H. Xu, J. Appl. Polym. Sci. **111**, 2648 (2009)
43. H. Xu, B. Yang, J. Wang, S. Guang, C. Li, J. Appl. Polym. Sci. **45**, 5308 (2007)